

THE FLARE KERNEL IN THE IMPULSIVE PHASE

(Invited)

Cornelis de Jager

Laboratory for Space Research, Utrecht, the Netherlands

ABSTRACT

The impulsive phase of a flare is characterized by impulsive bursts of X-ray and microwave radiation, related to impulsive footpoint heating up to 50 or 60 MK, by upward gas velocities (150 to 400 km s⁻¹) and by a gradual increase of the flare's thermal energy content. These phenomena, as well as non-thermal effects, are all related to the impulsive energy injection into the flare. The available observations are, also quantitatively, consistent with a model in which energy is injected into the flare by beams of energetic electrons, causing ablation of chromospheric gas, followed by convective rise of gas. Thus, a hole is "burned" into the chromosphere; at the end of the impulsive phase of an average flare the lower part of that "hole" is situated about 1800 km above the photosphere. H α and other optical and UV line emission is radiated by a thin layer (\approx 20 km) at the bottom of the flare kernel. The upward rising and outward streaming gas cools down by conduction in about 45 s. The non-thermal effects in the initial phase are due to curtailing of the energy distribution function by escape of energetic electrons. The single flux tube model of a flare does not fit with these observations; instead we propose the spaghetti-bundle model. Microwave and gamma-ray observations suggest the occurrence of dense flare knots of \sim 800 km diameter, and of high temperature. Future observations should concentrate on locating the microwave/gamma-ray sources, and on determining the kernel's fine structure and the related multi-loop structure of the flaring area.

I. MAIN CHARACTERISTICS OF THE IMPULSIVE PHASE

There are four main characteristics of the impulsive phase. The impulsive phase of a solar flare is primarily defined as the period of a few to ten minutes during which *impulsive bursts* of hard X rays (\gtrsim 20 keV) and of microwave radiation are emitted. There is a hierarchy of impulsive bursts, starting with the *burst complexes*, each of which last for about one or two minutes (Figure 1). These consist each of a few to some ten shorter lasting bursts, the *elementary flare bursts* (De Jager and De Jonge, 1978) which lasts for about 5 to 15 seconds each. These, in turn, can consist of still shorter lived bursts, the *sub-second pulses* (Kaufmann et al., 1980; Orwig, Frost, and Dennis, 1981) which are observed both in hard X rays and in cm-mm radio-waves. If observed simultaneously in both wavelength regions they appear to be synchronous down to the accuracy of the measurements (Takakura et al., 1983).

Imaging observations in X rays by means of the Hard X-Ray Imaging Spectrometer aboard SMM (Van Beek et al., 1980) have shown that the hard X-ray bursts are emitted by small localized areas, the *footpoints* or *flare kernels* (Hoynig et al., 1981). These footpoints occur often in pairs, and are then localized at either side of the magnetic inversion line (the "neutral line"), an observation that supports the flux tube model of a flare. Although the footpoints are principally visible in hard (\gtrsim 15 keV) X rays they can also be detected with about the same intensity in X rays of smaller photon energy (\approx 5 keV) if sufficient care is taken to subtract the gradual X-ray background flux (De Jager and Boelee, 1984; De Jager, Boelee, and Rust, 1984); cf. Figure 2. Apparently, the footpoints, although not a specific characteristic of the hard X-ray component, are very significant for the impulsive phase, because they occur only during the emission of the burst complexes.

Very characteristic for the early part of the impulsive phase are the upward motions (Antonucci and Dennis, 1983; Antonucci, Gabriel, and Dennis, 1985) with observed velocity components of 150 to 400 km s⁻¹, values derived from X-ray spectral data. The upward motions start rather suddenly at the very onset of the impulsive phase and they decrease with time, quasi-exponentially, with a typical e-folding time of one to a few minutes; cf. Figures 3 and 4. These motions are ascribed to the upward convection of hot gas, originating by ablation of the chromosphere through heating by incident electron beams, or by a hot plasma front.

During the impulsive phase the *thermal energy content* of the X-ray emitting component of the flaring region *increases steadily* (De Jager and Boelee, 1984; Antonucci, Gabriel, and Dennis, 1985) until the last X-ray burst has terminated; cf. Figures 4 and 5. The burst signature is absent in the $E_{th}(t)$ relation which shows that the temporal behavior of the energy input, which occurs through the impulsive bursts, is smoothed out. We will see later that this is caused by the way gas is streaming convectively from the kernel into the surrounding area, the flare tongue, which is the region responsible for the emission of the gradual phase component.

The four aspects listed above: impulsive bursts, footpoints, convective motions, and energy input, are the main characteristics of the impulsive phase.

II. PHENOMENOLOGY AND SCENARIO OF FLARE KERNEL HEATING

An important aspect of the first part of the impulsive phase of flares with essentially one of at most two impulsive burst complexes is that the Doppler temperature derived from line broadenings of X-ray spectral lines becomes abruptly high at the onset of the impulsive phase (Antonucci, Gabriel, and Dennis, 1985; Figure 5). Within a minute it appears to rise to about 5×10^7 K or higher, to decrease slowly, and quasi-exponentially thereafter. With an e-folding time of 1.5 min it approaches the electron temperature derived from line intensity ratios. The temperature derived from the count-rate ratios in the medium-energy HXIS channels (≈ 16 keV) shows the same behavior (Figure 6). The Doppler-temperature is an ionic temperature because it is derived from the thermal, or in any case, from the stochastic motion field of the ions. But it is at the same time an electron temperature, because the electron-ion exchange time in the kernel plasma is short, of the order of 0.1 s, so that a thermal energy distribution establishes rapidly. There is, however, one reserve. The average energy of electrons of 5×10^7 K is ≈ 5 keV, while the kernel area is transparent for electrons with $E \gtrsim 15$ keV, so that the tail of the electron energy distribution curve cannot form. The excitation and ionization of the gas ions is determined by the high-energy electrons, hence by the tail of the electron energy distribution function. This is the reason why the electron temperature derived from the line intensity ratios, and also the one derived from count-rates ratios in low-energy (3 to 10 keV) HXIS channels, is lower than the temperature derived from count-rate ratios around 16 keV, and also lower than the ionic Doppler temperature: the latter is defined by the main (average) part of the energy distribution curve.

The transparency of the kernel for particles with $E \gtrsim 15$ keV is also the reason why the high temperature in the early part of the impulsive phase must be due to heating of electrons with energies $\gtrsim 15$ keV: under standard kernel conditions only these can penetrate through the kernel and heat the underlying chromosphere.

From an analysis of the X-ray and XUV observations of two flares with essentially one burst-complex (8 April and 5 November, 1980) the present author (De Jager, 1985b) has derived a model of a flare kernel as shown in Figure 7. This model describes the flare kernel at the end

of the ablation process, hence at the end of the impulsive phase: heating of the chromosphere by bombardment with electron beams with $E \gtrsim 15$ keV causes ablation of the chromosphere. At the end of the impulsive phase the bottom of the kernel "hole" has decreased to a height of ≈ 1800 km above the chromosphere. There, the normal chromospheric particle density is $\approx 10^{13}$ cm $^{-3}$. At the transition between chromosphere and kernel a thin (≈ 20 km) layer of particles with $T_{el} \approx 10^4$ K forms, emitting H α and other low energy lines. This layer is heated to 5×10^7 K in about 10 s and is replaced by new material through continuous ablation. The ablated particles move upward convectively with velocities of ≈ 150 to 400 km s $^{-1}$. Since the kernel has a depth of ≈ 2500 km this heated gas takes 8 to 10 s to reach the "top" of the chromosphere. During the impulsive phase a "dome" of superhot gas is formed over the kernel. This dome contains about four times more particles than the kernel proper (see Figure 3), but its gas content has mainly a horizontal velocity component, with a possible structure as suggested in the insert to Figure 7. Guided by magnetic field lines, assumed vertical in the kernel, and fanning out into the "dome" and beyond (the "spaghetti-bundle model") it takes the plasma about 45 s to cool down conductively to the ~ 20 MK temperature, characteristic for the gradual phase component. The conduction time of 45 s is equal to the time gas needs with $v = 200$ km s $^{-1}$ to move along the field lines through kernel and dome.

The kernel model, described here, consistently unites the XRP spectral observations of line intensity ratios, line broadening and displacement and the data on heating and temperature derived from HXIS and HXRBS data. As will be shown in Section IV this is also true quantitatively.

III. CORONAL EXPLOSIONS

Coronal explosions are a feature discovered by De Jager and Boelee (1984), and are further described by De Jager, Boelee, and Rust (1984), De Jager (1985a), and De Jager and Lemmens (1985). Figure 2, lower part, shows the explosion observed in the flare of 12 November 1980, 02:50 UT.

The coronal explosion is a density wave originating from a small area near to, or identical with, the flare's footpoints. The waves propagate with initial velocities of the order of a few hundred to more than a thousand km s $^{-1}$, a velocity which normally decelerates rapidly to values below 100 km s $^{-1}$. The explosion shown in Figure 2 has an initial lateral velocity component of 200 km s $^{-1}$ which slowed down to 20 km s $^{-1}$ in some two minutes. It started just after the last hard X-ray burst complex, cf. Figure 1.

The most probable explanation for these observations is that the explosion shows the lateral displacement of the plasma escaping from the kernel, guided by the magnetic field line pattern emanating from the kernel area, as suggested by the schematic drawing in the insert to Figure 7.

IV. NUMBERS AND ENERGIES

We summarize some typical values, derived from observations of the flares of 8 April and 5 November 1980.

Number of particles ablated (De Jager, 1985b):

Per second for the whole kernel: $4 \times 10^{36} \text{ s}^{-1}$

During the whole impulsive phase for the whole kernel: 3.5×10^{38}

During the whole impulsive phase, per cm^2 : $3.2 \times 10^{20} \text{ cm}^{-2}$.

Next we summarize values for the time integrated energies over the impulsive phase:

Energy of incident electron beam $> 25 \text{ keV}$ (Dennis et al., 1985): $6 \times 10^{30} \text{ erg}$

Energy of incident electron beam $> 16 \text{ keV}$ (De Jager, 1985b): $13 \times 10^{30} \text{ erg}$

Energy of convective motions (Antonucci, Gabriel, and Dennis, 1985): $7 \times 10^{30} \text{ erg}$

Maximum thermal energy content of gradual phase component (Dennis et al., 1985):

$2.6 \times 10^{30} \text{ erg}$

Energy needed to heat 20 km thick layer ($n_e = 10^{13} \text{ cm}^{-3}$) to 50 MK (De Jager, 1985b):

$3.6 \times 10^{30} \text{ erg}$.

These energy values are internally consistent and support the ablation-convection model.

V. MICROWAVE AND GAMMA-RAY OBSERVATIONS

These may yield important information on the – relatively – high density phenomena in flares. Microwave observations made at the highest frequencies (90 MHz) by Kaufmann et al. (1985a) demand an interpretation in terms of source densities of the order of $n_e \approx 10^{14} \text{ cm}^{-3}$ (Kaufmann et al., 1985b) and source sizes of $\approx 800 \text{ km}$ diameter. Their temperatures should be high, above 10^8 K . Also gamma-ray observations suggest source densities of that order (Chupp, 1984).

On the basis of the model shown in Figure 7 we therefore suggest that these sources are situated just below the flare kernel's base, in the dense parts of the chromosphere, at some 500 to 1500 km above the photosphere. The effects of flare heating by sources at that level need to be investigated and form an interesting challenge to theorists, as well as to observers who should locate these sources and determine their precise sizes.

VI. REQUIREMENTS FOR FUTURE RESEARCH: OBSERVATIONAL AND THEORETICAL

The model of the flare kernel described in Section II is a static model while a kernel is a dynamic feature. In its very beginning, when the hot ($n_e = 10^{11} \text{ cm}^{-3}$) gas has not yet formed, heating and ablation of the chromosphere is easier than later. In the course of the ablation process a high plasma pressure is built up ($\approx 10^3 \text{ dynes cm}^{-2}$) which pushes the $\text{H}\alpha$ emitting region downward; this explains the observed downwards velocities in $\text{H}\alpha$ and other spectral lines. In addition, ablation “burns” a hole into the chromosphere, which, at the end of the impulsive phase, results in a structure outlined in Figure 7.

A first theoretical problem to tackle is the dynamic time development of the flare kernel. Another theoretical problem is that of the non-thermal character of the electron energy distribution in the kernel. Curtailing of the electron energy distribution curve by escaping electrons (as described in Section II) may lead to a significant difference between the ionic Doppler temperatures and the electron temperatures derived from low-energy count rate ratios or from line intensity ratios.

Observationally the solution of the following problems seems essential for further progress in the understanding of solar flares. The observation that the gradual component of flares is not confined to a single loop (as assumed in the classical flare picture) but to a large volume with a very small filling factor ($\approx 10^{-2}$) suggests the “spaghetti-bundle” model for the flare area. This model must also demand a considerable fine structure of the flare kernel seen from above. Hence it is worth investigating (a) if the kernel area ($\approx 10^8 \text{ km}^2$) has a fine structure, and (b) if the gradual phase component consists of many loops, corresponding to the footpoints in the fine-structure of the kernel. In addition, it is of importance to examine if the propagation of the density waves related to the coronal explosions is associated with shock-wave phenomena such as the existence of a thin layer of temperature enhancement near the shocks.

One of the most important topics for future research seems the observation of the high temperature, high density, flare knots whose existence is suggested by extreme microwave and by gamma-ray observations. Are these knots really situated below the flare kernel and if so, at what level; what are their densities and sizes. Solution of this problem may be fundamental for further progress in our understanding of solar flares.

REFERENCES

- Antonucci, E. and Dennis, B. R., 1983, *Solar Phys.*, 86, 67.
Antonucci, E., Gabriel, A., and Dennis, B. R., 1985, in press.
Chupp, E. L., 1984, *Ann. Rev. Astron. Astrophys.*, 22, 359.
De Jager, C., 1985a, *Solar Phys.*, 96, 143.
De Jager, C., 1985b, *Solar Phys.*, accepted.
De Jager, C. and Boelee, A., 1984, *Solar Phys.*, 92, 227.
De Jager, C. and De Jonge, G., 1978, *Solar Phys.*, 58, 127.
De Jager, C. and Lemmens, A., 1985, *Solar Phys.*, in preparation.
De Jager, C., Boelee, A., and Rust, D. M., 1984, *Solar Phys.*, 92, 245.
Dennis, B. R., Kiplinger, A. L., Orwig, L. E., and Frost, K. J., 1985, NASA Technical Memorandum 86187.
Hoyng, P., and 11 co-authors, 1981, *Astrophys. J. (Letters)*, 246, L155.
Kaufmann, P., Strauss, F. M., Opher, R., and Laporte, C., 1980, *Astron. Astrophys.*, 87, 58.
Kaufmann, P., Correia, E., Costa, J. E. R., Zodi Vaz, A. M., and Dennis, B. R., 1985a, *Nature*, 313, 380.
Kaufmann, P., Correia, E., Costa, J. E. R., and Zodi Vaz, A. M., 1985b, *Astron. Astrophys.*, in preparation.
Orwig, L. E., Frost, K. J., and Dennis, B. R., 1981, *Astrophys. J. (Letters)*, 244, L163.
Takakura, T., Kaufmann, P., Costa, J. E. R., Degaonkar, S. S., Ohki, K., and Nitta, N., 1983, *Nature*, 302, 317.
Van Beek, H. F., Hoyng, P., Lafleur, B., and Simnett, G. M., 1980, *Solar Phys.*, 65, 39.

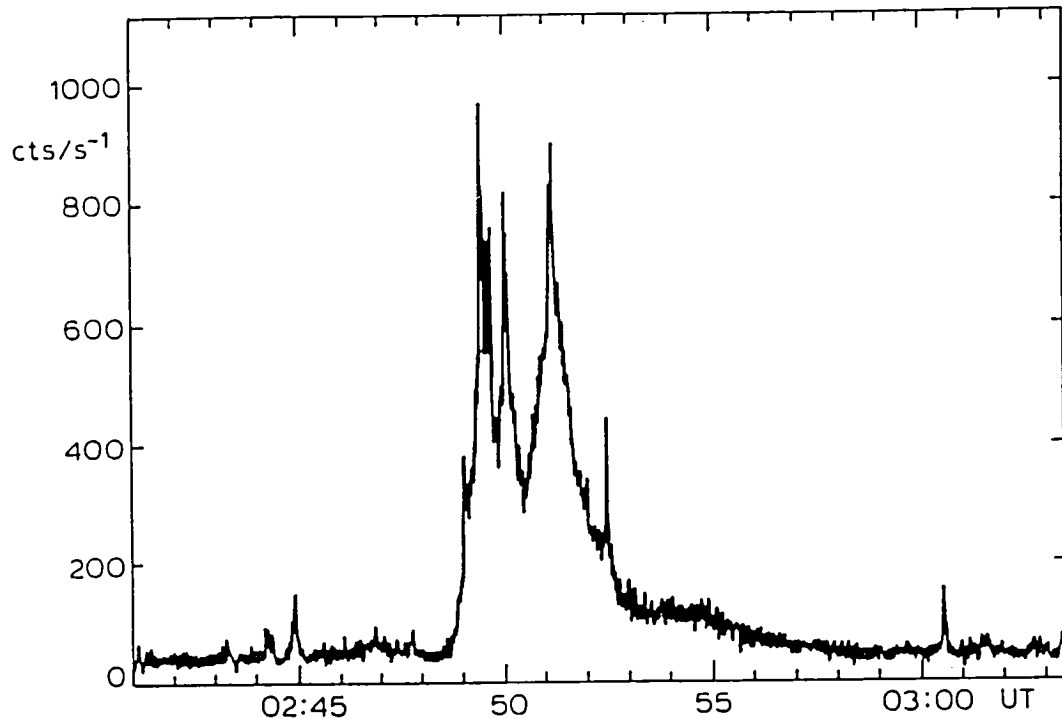


Figure 1. Impulsive bursts of the flare of 12 November 1980; 02:50 UT. The main burst complex is at 02:49-:51 UT. There are earlier weaker bursts; those at 02:44 UT and 02:45 UT mark the start of the flare (HXRBS observations, by courtesy of B. R. Dennis; see De Jager and Boelee, 1984).

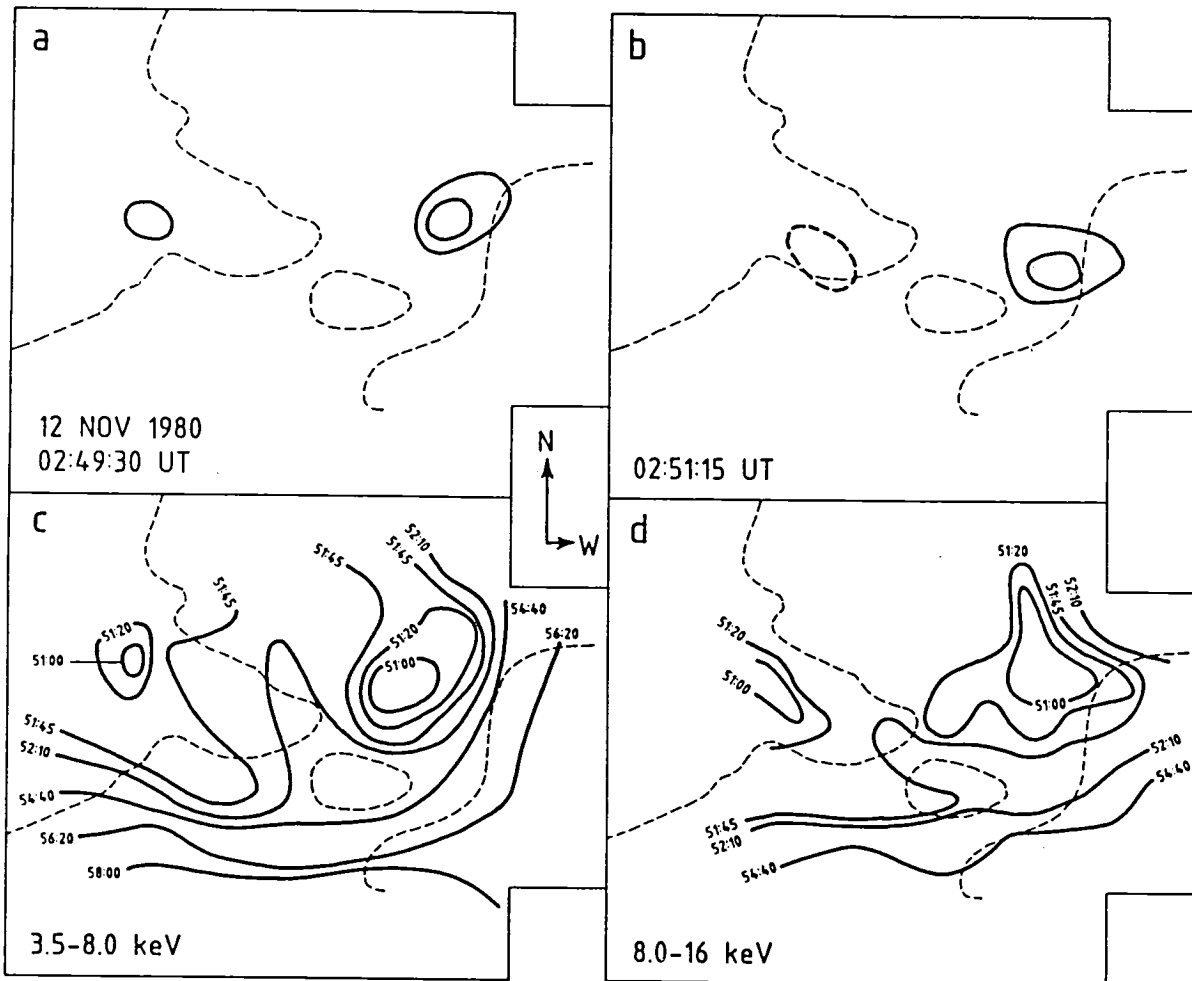


Figure 2. Upper part: even low-energy X-ray observations of flares show the footpoints, but only at the time of the hard X-ray bursts, and only after careful background subtraction (De Jager and Boelee, 1984; De Jager, Boelee, and Rust, 1984). The lower part shows the coronal explosion associated with this flare (see Section III) in two energy ranges. The lines are isochrones, labeled with the time in minutes and seconds after 12 November 1980, 02:00 UT. In all four figures the dashed line is the inversion line. For other data relevant to this flare see Figures 1 and 5.

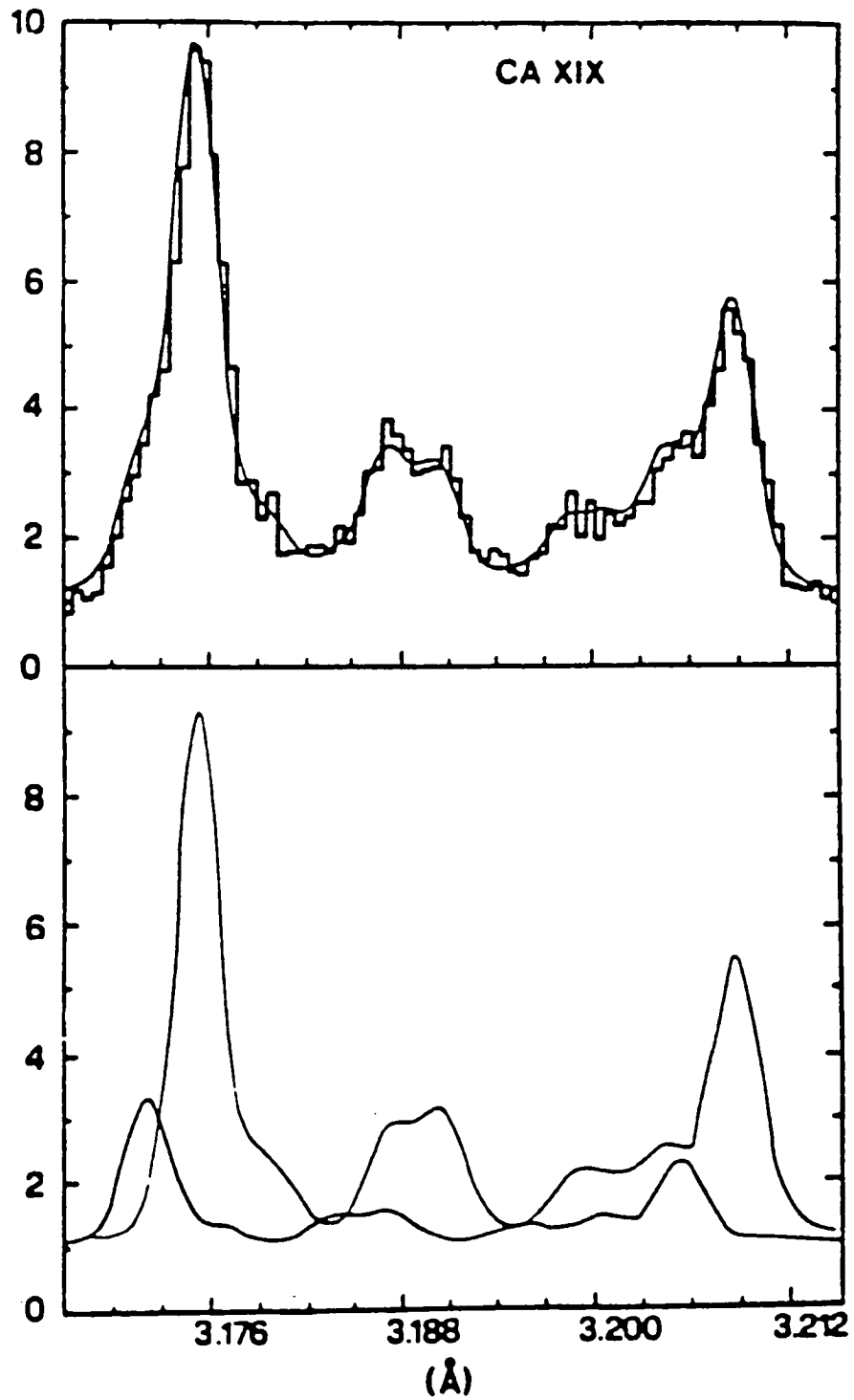


Figure 3. Convective velocities in flare kernels are derived from line displacements in X-ray spectra. About one-fifth of the hot material shows upward displacement; the rest is stationary (Antonucci, Gabriel, and Dennis, 1985).

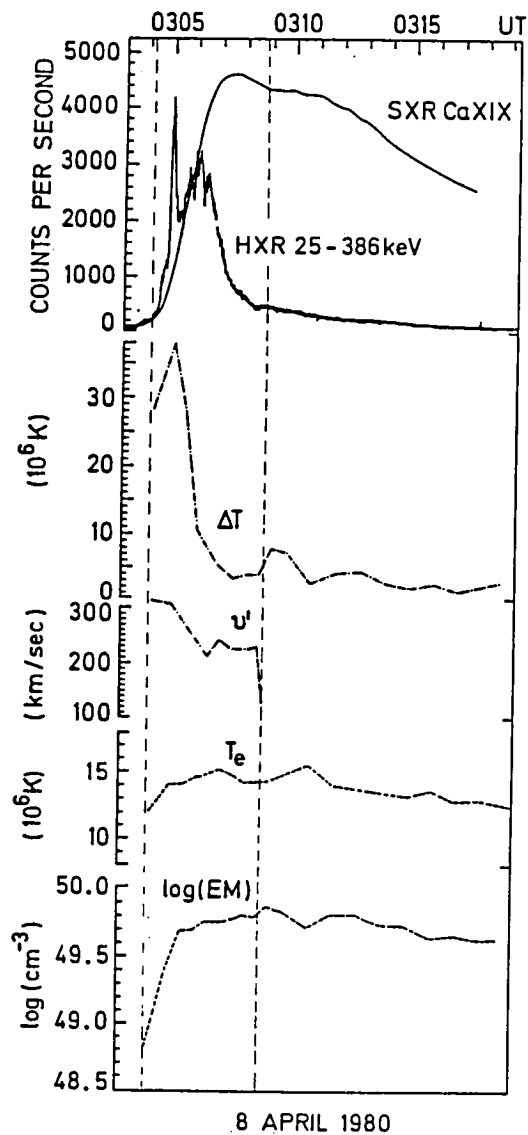


Figure 4. Phenomena in the impulsive phase of the flare of 8 April 1980; 03:50 UT. The upward velocities (v') increase abruptly to high values at the start of the impulsive phase, to gradually decrease afterwards. Note also the relation with the impulsive hard X-ray burst complex, and with ΔT_D (XRP observations; Antonucci, Gabriel, and Dennis, 1985).

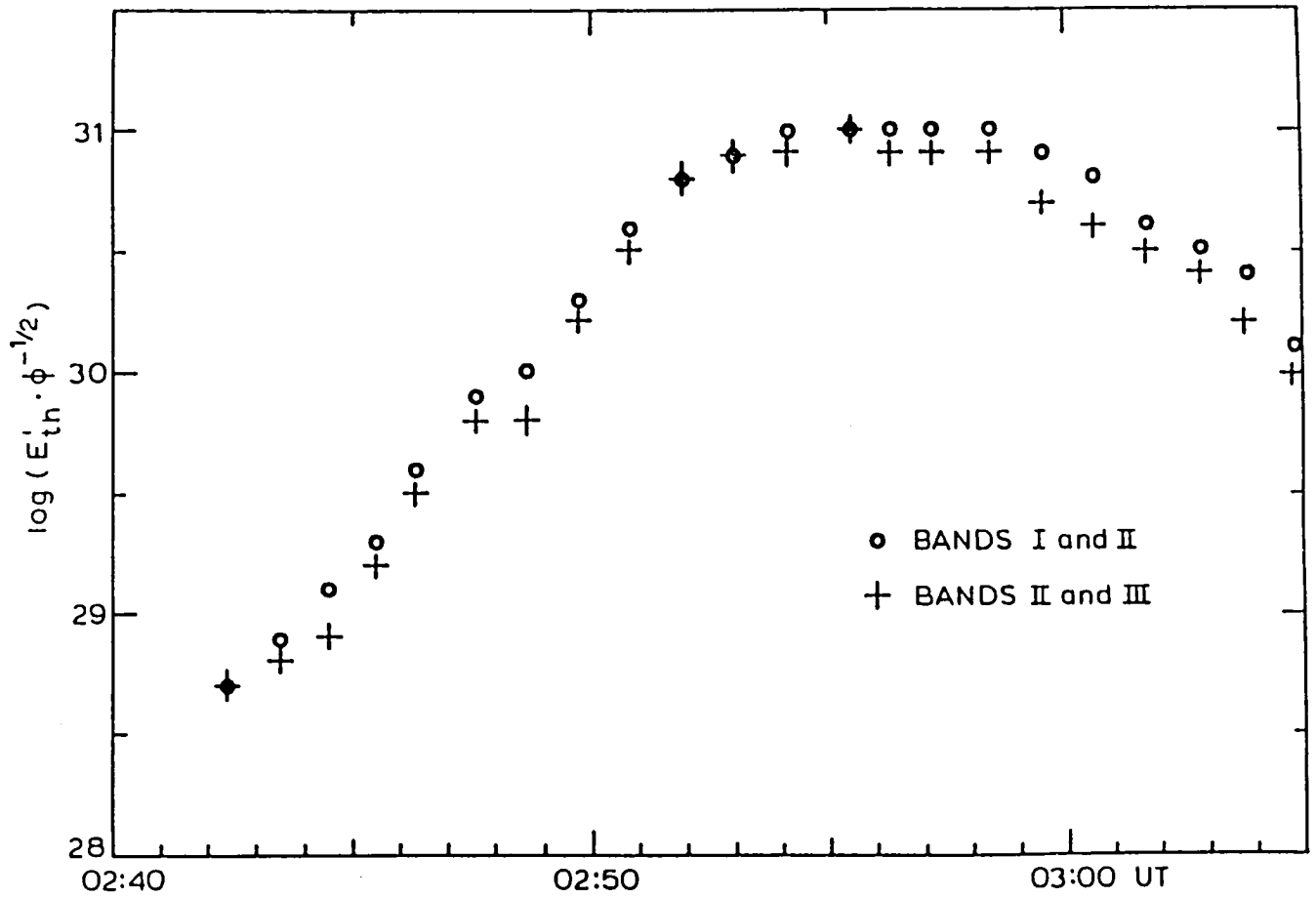


Figure 5. Thermal energy content of a flare increases gradually and reaches a maximum at the end of the impulsive phase (De Jager and Boelee, 1984). Here, ϕ is the filling factor, $\approx 10^{-2}$.

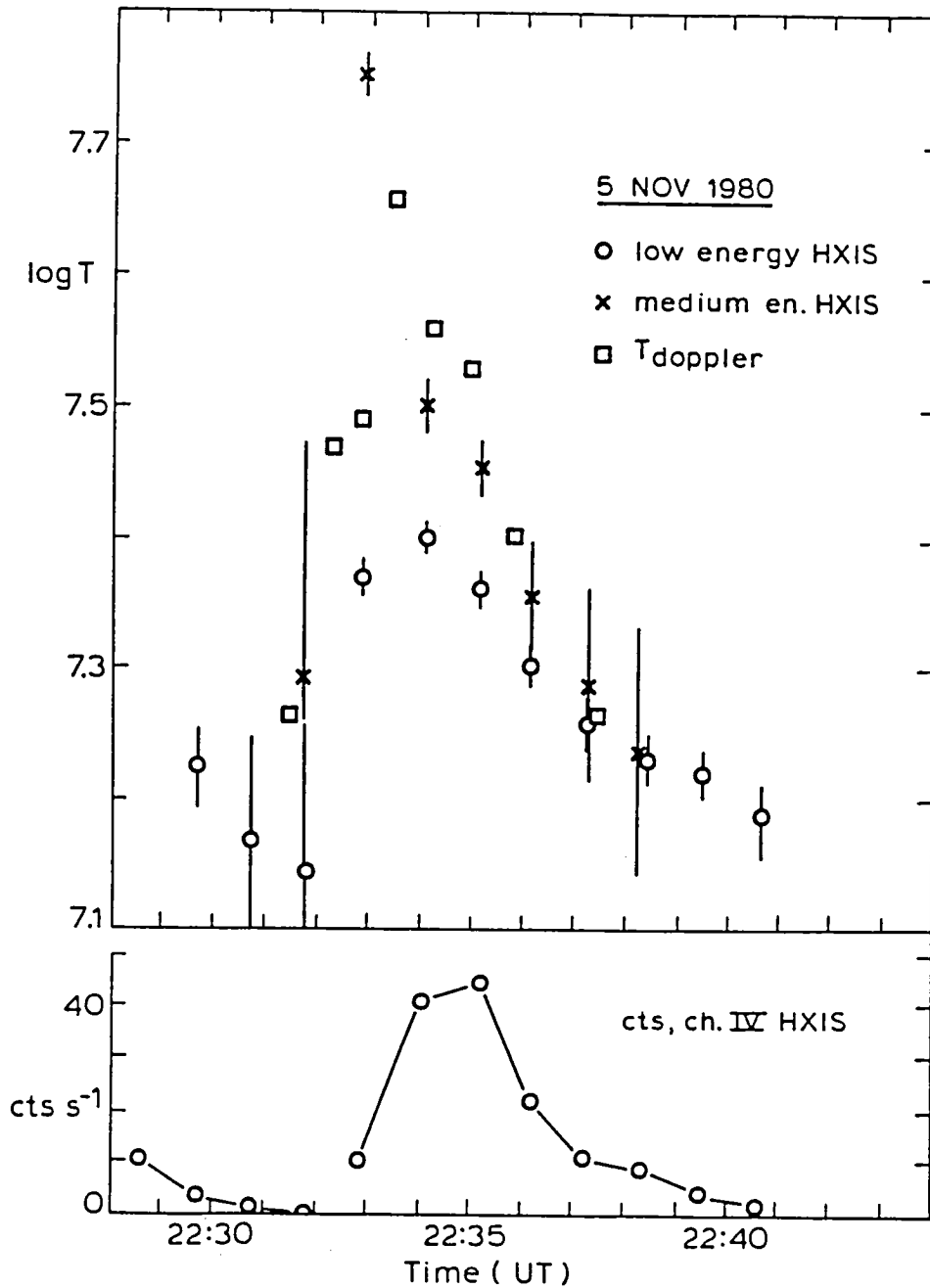


Figure 6. Non-thermal effects in the impulsive phase. At the flare's onset the temperature derived from line broadening, and the one derived from medium-energy HXIS count rates (≈ 16 keV) rise abruptly to ≈ 50 MK, to decrease quasi-exponentially thereafter, with an e-folding time of 1.5 min. The electron temperature, derived from line intensity ratios, and the temperature derived from low energy HXIS count-rate ratios increases too, but less. After a few minutes all temperatures are equal. The lower part of the figure shows the count rate in HXIS channel IV (11 to 16 keV), to give an impression of the time-development of the impulsive phase (De Jager, 1985b).

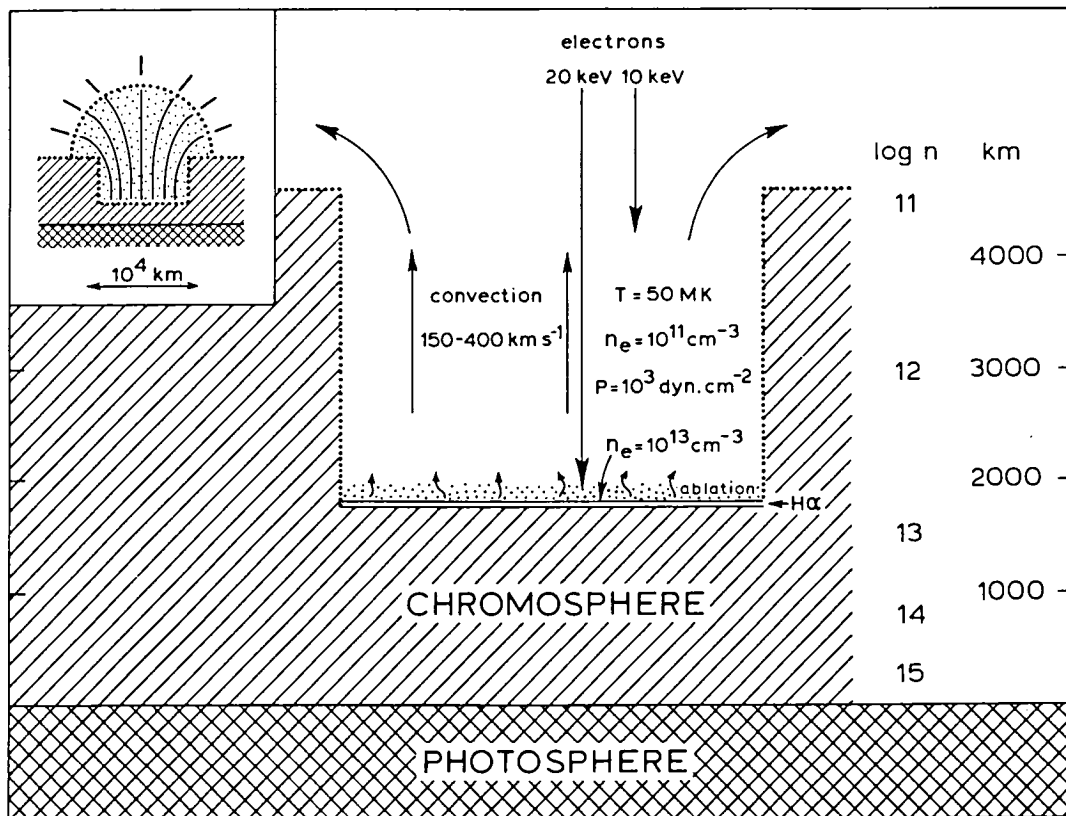


Figure 7. Model of a flare kernel at the end of the impulsive phase of an average flare. Electron beam bombardment followed by ablation has “burned a hole” in the chromosphere down to a level about 1800 km above the photosphere. The gas in this hole has $T \approx 50$ MK, $n_e \approx 10^{11} \text{ cm}^{-3}$, $P \approx 10^3 \text{ dynes cm}^{-2}$. Gas streams up and outward (see the insert) with $v = 150$ to 400 km s^{-1} . $H\alpha$ and other optical line radiation is emitted by a 20 km thick layer at the bottom of the kernel (De Jager, 1985b).